

A Biologically Based Flight Control System for a Blimp-based UAV

Sergi Bermúdez i Badia, Pawel Pyk and Paul F.M.J. Verschure

*Institute of Neuroinformatics
ETH / University of Zurich
Winterthurerstr. 190, CH-8057 Zurich, Switzerland
sergi@ini.unizh.ch*

Abstract - Autonomous navigation in 2D and 3D environments has been studied for a long time. Navigating within a 3D environment is very challenging for both animals and robots and a variety of sensors are used to solve this task ranging from vision or a simple gyro or compass to GPS. The principal tasks for 3D autonomous navigation are course stabilization, altitude and drift control, and collision avoidance. Using this basis, some features can be easily added like aerial mapping, object recognition, homing strategies or takeoff and landing. Here we present a biologically based control layer for an Unmanned Aerial Vehicle (UAV) that provides course stabilization, altitude and drift control, and collision avoidance. The properties of this neuronal control system are evaluated using a flying robot.

Index Terms – Visual Navigation, UAV, Elementary Motion Detectors, insect visual system, neuronal model, flying robot.

I. INTRODUCTION

Many UAVs (Unmanned Aerial Vehicles) are and have been used to handle the 6 degrees of freedom that the real world imposes, most of them are either helicopter or blimp based [1][2][6][11][12][17][27][28]. A helicopter based UAV might be more attractive than a blimp based one, but it requires dealing with some complicated handicaps. Some helicopters based UAVs are gasoline powered and have a short flight time. Since these UAVs are model sized, the time constants describing their dynamics are very short, and therefore these devices are unstable. This means that in order to solve the stabilization problem one is obliged to use inertial sensors [1][2][12][17]. For these reasons we use a dirigible.

The use of specific sensors for basic navigation tasks implies that methods or systems must be developed to process their data and perform the actual control task. Some algorithms for visually guided navigation, in order to reduce the need for additional specialized sensors, use optimization approaches such as evolutionary algorithms; they require a training period to adapt to their interaction with the environment relying on algorithms that have high working memory and processor time requirements [11][31][32].

These approaches are quite complex compared to what actually happens in nature, where the sensor processing and behavioral control systems implemented by brains of about 1mm^3 and consisting of less than 10^6 neurons cannot be assumed to be able to perform such complex computations or actually survive long enough to go through the required training period.

Here, we focus on directly investigating and reconstructing the principles underlying biological navigation systems. Of particular interest is the insect flight control system because of its ability to show a robust response using relatively simple mechanisms to control flight course, avoid collisions, secure takeoff and landing and so on. In this field a lot of work has been done including obstacle avoidance, homing and trajectory following using ground based, terrestrial robots operating within 2D environments [18][19][21][31][32]. Using ground bound mobile robots provides for a simplified version of the problem that flying insects solve. The latter negotiate a complex dynamics that include inertia and 6 degrees of freedom that lead to problems of course stabilization and position control that ground based systems do not face.

Many projects investigating insect based (fly and bee) models for course stabilization have reasonably good results relying on vision, although occasionally biologically unrealistic sensors are included [11][20]. For obstacle avoidance, however, the situation is different. Here only few models have been proposed and applied to mobile robots. So far none of these have been tested on UAVs [6][11][28].

II. METHODS AND MATERIALS

A. Setup

We have developed a blimp-based robot designed to work within indoor environments (fig. 1). The dimensions of the hull are 30 cm of radius and 120 cm of length that provides a payload of about 250 gr. at 600 meters over sea level. The robot is powered using a Lithium-Polymer battery of 10 gr. that can provide for about one hour of autonomous flight at maximum speed (*West-technik, Germany*). Four

* This research is supported by the European community and BBW (Grant "A Fleet of Artificial Chemosensing Moths for Distributed Environmental Monitoring (AMOTH)" to PFMJV, funded under the IST Future and Emerging Technologies Programme (IST-2001-33066, www.amoth.org)

propellers are mounted in a balsa wood structure providing the robot with independent control for altitude and translation. The propellers are hand made and tuned to take the most of our motors with 1:4 gearboxes, providing 20 gr. thrust per motor at full speed (*Didel, Switzerland*).

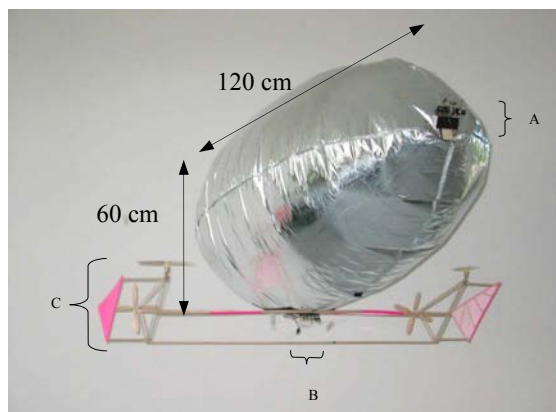


Figure 1: General characteristics of the UAV. A) 2 CCD color cameras with PAL transmitters; B) Main board with radio receiver and battery; C) Custom propellers specifically tuned for the motors and gearboxes.

The UAV is equipped with two CCD color cameras mounted on the front part (*“Module 3”, Conrad Electronics, Switzerland*), pointing to the left and right sides respectively separated by 110°. These lightweight high-resolution cameras (628[H] x 582 [V] pixels) are equipped with wide-angle lenses (*2.5 mm lenses, Conrad Electronics, Switzerland*) that provide the visual input to control model. Given the opening angle of the cameras of 100[H] x 87[V] degrees the combined camera system covers over 180 degrees of the frontal horizontal sphere. The images acquired with the cameras are sent via two lightweight PAL transmitters (*SDX-21LP video transmitters working at 2.4 GHz band, produced by RF-Video, Canada*) to our ground station where they are processed. A radio receiver connected to the on-board control board allows the control of the speed of all the motors separately via a radio link.

The ground station setup consists of two PAL receivers (*Wavecom, produced by RF-Video, Canada*) that receive the signal from the cameras; a quad combiner (*Grand Virtual Guard, ARP Datacon*) that puts them together in just one image; and a USB frame grabber (*Liferview USB Capview, Liferview, Taiwan*) is used to acquire the image. The image is processed in IQR421 [29], a neural simulator software that runs on a laptop computer under Linux. IQR421 allows the user to define large-scale real-time neuronal models that can be interfaced to real-world devices. All ground station programs providing the interfaces between the UAV and IQR421 run at about 50 Hz. After the processing of the data by our models, an action is decided and transmitted to the UAV. This action is sent as a command to the motors via a radio transceiver connected to the serial port of the computer. The digital link is capable to transfer data between the ground station setup and the UAV in real time.

The communication is established using a pair of BIM433-F transceivers (*Wireless World AG, Switzerland*), allowing up to 115200 bauds for serial communication.

B. Tracking system and data analysis

In order to analyze and quantify the trajectory and the behavior of the UAV accurately, we have developed a tracking system. This tracking system is designed for 3D tracking in real time and provides us with the position (x,y,z) , heading direction (x_h,y_h,z_h) and linear velocity of the UAV. Furthermore, this data is acquired synchronously with the responses of the neural model that controls the flight behavior. Hence, we are able to directly relate the states of the neuronal control system to the behaviours of the UAV.

The experiments are performed in a 4 X 4 meters room with randomly distributed solid black squares on the walls and the floor as visual cues (fig. 2). On the top of this room a tracking system is mounted consisting of two infrared cameras equipped with wide-angle lenses (*2.5 mm lenses, Conrad Electronics, Switzerland*) that make use of stereoscopy in order to track two IR LED's mounted on top of the hull of the UAV.

The transformation of the two camera pixels coordinates into a pair of three dimensional position points is achieved with a multilayer perceptron. A large amount of pre-mapped points in the room are used as reference points for interpolation. The tracking resolution achieves an accuracy of up to 5 cm. The acquisition is performed at 5Hz and the data analyzed using Matlab (*Mathworks, USA*) and IQR421 [29].

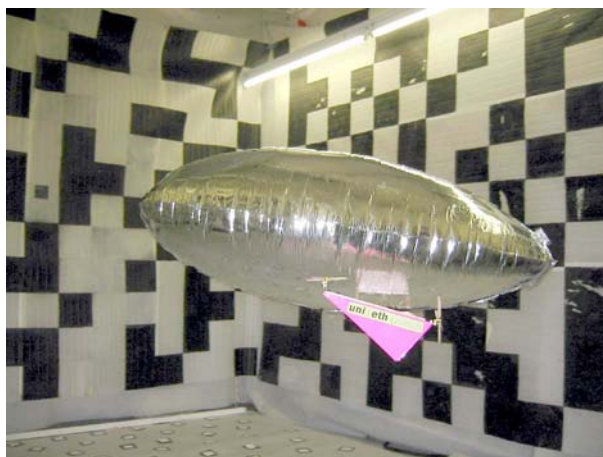


Figure 2: Image of the UAV flying in our blimpodrome. The walls and the floor of the 4x4 meters room are covered with randomly distributed black squares to provide visual cues to the UAV. The tracking system is mounted at the ceiling of the room, providing us with the position, orientation, and velocity of the UAV at every moment in time.

III. MODELS

Course stabilization and collision avoidance is derived from insect based neuronal models, and consequently, they model several processes performed in different layers of the insect visual system. The first steps of image processing in the insect visual system relevant to our tasks are the normalization of the image (logarithmic compression of the response of the photoreceptors) and a contrast enhancement (center/surround antagonism). These first processes provide the system with robustness to changes in the luminance level and also reduce the redundancy in the input and occur also in the fly's lamina neuronal layer [30].

After the extraction of the relevant contrast information the models independently process this information (fig. 3) to extract stabilization or collision cues. The output connections from both processing streams project onto the optomotor group that decides upon the action that has to be sent to the UAV. Therefore, this group translates the responses of the neuronal models into commands for the UAV. These commands are processed at two different priority levels: stabilization responses are inhibited whenever a collision is detected that results in an avoidance action.

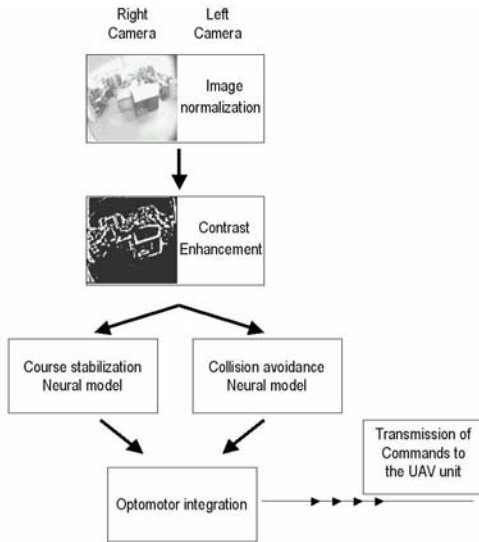


Figure 3: General structure and interconnection of the two visual streams of our model. This schema shows the different layers of the neuronal control system: After a common input stage, the implemented streams work in parallel and they both project onto the optomotor group. The optomotor group decides upon the next action to perform, The state of this neuronal population is readout by the interface software and the motor commands are sent to the UAV.

A. Course Stabilization and drift compensation

Trying to imitate the simplicity and effectiveness of insect systems, we have modeled the fly stabilization system combined with the collision avoidance system of the locust. The model presents a similar response to the stimulus compared to a HS or VS cell of the visual system of the fly, these cells are motion sensitive and respond maximally to a

stimulus in their preferred direction and minimally in their null direction (opposite sense) [4][5]. Both HS and VS cells are output neurons of the visual system believed to be involved in providing relevant visual information that is used in course control. These cells are believed to encode the direction of rotation of the animal largely independent of the spatial layout and texture of the environment [10]. Only when the animal is very close to an object, the neural responses are affected by it [14][15].

The stabilization behavior of flies is dependent on the optic flow that they detect and based on their optomotor behavior the formal “correlation model” of local movement detectors was proposed already long ago [23]. Just a few elaborations have to be performed in order to adapt this correlation model to reflect the specific features of the fly's motion detection system [5].

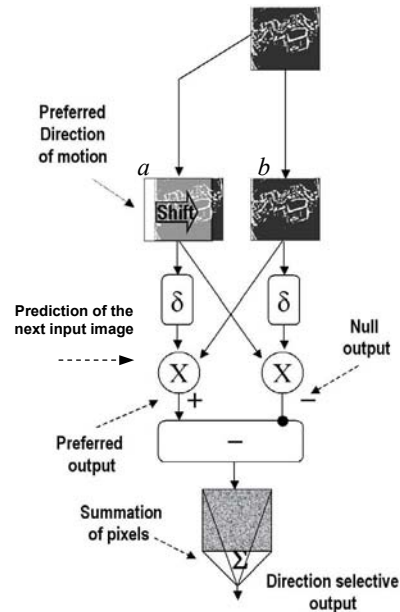


Figure 4: The EMD implementation, making use of the Reichardt correlator [22], where δ represents a delay, X the multiplication operation and $-$ the subtraction operation. In this case, the preferred direction of motion is rightward.

The model makes use of two inputs corresponding to the intensity given by two photoreceptors (a and b in fig. 4) separated by a certain distance D . There are two branches, the null and preferred outputs, which are computed independently. Given a translating object from a to b at a certain speed v :

$$Output_{Preferred} = I_a(t-\delta) * I_b(t), \quad (1)$$

$$\text{where } I_b(t) = I_a(t-D/v)$$

$$\text{then } Output_{Preferred} = I_a(t-\delta) * I_a(t-D/v), \quad (2)$$

The closer D/v is to δ , the higher the preferred output is; and therefore, the closer D/v is to $-\delta$, the higher the null output is. The addition of both preferred and null branches results in a directional selective response.

The, so called, Reichardt correlation model is used to assess the direction of movement of the image and, hence, of the UAV (fig. 4). To detect whether the UAV is moving in the preferred direction, a “correlation” is calculated between the current image and a prediction of the image for a movement performed in that direction. The prediction is obtained shifting the current image into the desired direction and storing it. Thus, by multiplying our prediction with the next input image we can obtain a parameter of similarity between them, which will allow us to say whether the motion was performed in that direction or not, and the extent of this movement. This implementation of correlation is applied at the level of image pixels; every pixel drives one, so called, Elementary Motion Detector (EMD) and for every pixel a correlation is computed to assess the optic flow (fig. 4).

The basis of our model is the Elementary Motion Detector (EMD) and every EMD is sensitive to motion in one direction. We have implemented four different preferred directions, as in flies [5][9], using a total of 625 pixels (25 x 25 layer) for the input image. The result is a system that detects horizontal and vertical motion in both directions.

In flies we can find about 60 motion sensitive tangential cell, including HS, VS and CH cells [9]. In the *Drosophila* there are about 800 ommatidia and there are 8 photoreceptors (R1-R8) dedicated per ommatidia [22]. In our implementation we use a slightly lower resolution, 25x25 input pixels (625 pixels) are used instead of the 800 ommatidia found in *Drosophila*. Every pixel in our input image corresponds to a single photoreceptor that gets the luminance level whereas in nature we find 8 photoreceptors per ommatidia [22]. In spite of the fact that flies have about 50–60 tangential cells (wide-field motion sensitive neurons) located in the lobula plate [9], our implementation only makes use of four wide-field motion sensitive neurons that are made up of the average response of those 25x25 local motion sensitive cells. Every one of the four EMDs used in our system is dedicated only to either the vertical or horizontal axis, and only sensitive to one direction [4][5][13][22][23]. The response of these cells is transmitted to the optomotor group. The optomotor group is the functional layer where all outputs of the two visual streams converge. The optomotor group generates the actions that will compensate for any drift of the UAV or allow it to avoid collisions. Each action is encoded by a single neuron of this population and winner-take-all competition among them provides for action selection. The states of the optomotor group are read-out by the interface software and packaged into a motor command that it transmits to the UAV.

B. Collision detection and obstacle avoidance

The model for collision avoidance is based on the locust visual system, where the, so called, Lobula Giant Movement Detector (LGMD) cell has been found: a wide-field neuron that responds to looming stimuli [7][8][25][26]. This cell responds to looming stimuli dependent on the velocity of the approaching object and the distance to this object, increasing its firing rate (activity) as the object approaches.

In previous work we have developed a model of the LGMD that was shown to allow a mobile robot to avoid collisions [18][19]. Here we present a further extension of this model to a complex 3D environment. As opposed to the previous model the current version assumes that also the LGMD receives inputs from motion sensitive cells of the Reichardt type in order to allow it to differentiate between expanding and contracting stimuli [3].

Since we have two cameras as sources of information, two LGMD neurons are implemented to detect looming, i.e. approaching, stimuli on each side of the visual field. Whenever a train of spikes is produced by one of the simulated LGMD cells, either left or right, it triggers an avoidance reaction in the opposite direction, performing a turn of variable angle depending on the strength of the response of the LGMD model. If both LGMD models respond at the same time to an approaching stimulus a reverse action is triggered. The responses of the collision detection models overwrite the responses of the stabilization model in order to prioritize avoidance reactions.

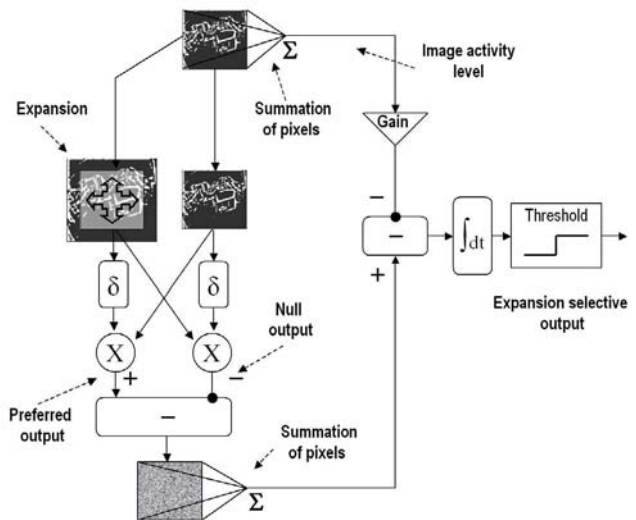


Figure 5: Implementation of the LGMD model, making use of the Reichardt correlator [22], where δ represents a delay, X the multiplication operation and $-$ the subtraction operation. This model responds to looming stimuli in the visual field taking into account that the strength of the response will depend on the global activity level of the image (feed forward inhibition), these specific and non-specific inputs are integrated over time and thresholded [3].

The LGMD model responds to looming stimuli, and to do so it calculates the similarity between the current input and a previous image, that is expanded. In addition the global activity level of the input image is taken into account. The LGMD cell triggers an avoidance reaction whenever a certain threshold is reached (fig. 5).

IV. RESULTS

A. Course stabilization and drift compensation

In order to evaluate the robustness and effectiveness of the model, a number of experiments are performed in our test room. The first evaluation is performed under ideal conditions, without wind or any controlled disturbance (fig. 6).

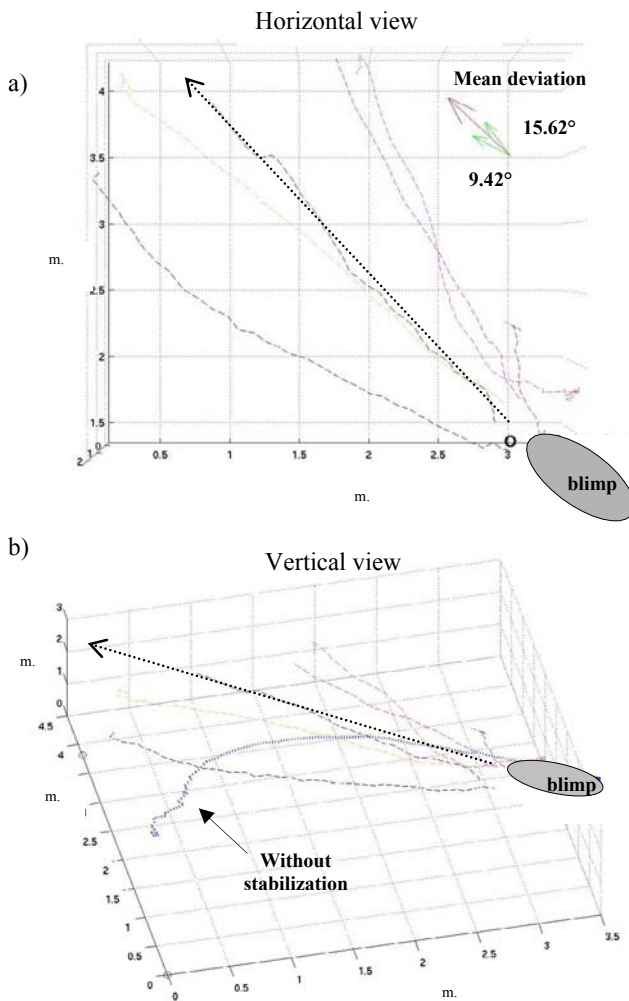


Figure 6: Traces of 6 test flights using the stabilization model. a) Horizontal and b) vertical view of the traces compared to the behavior without stabilization. The UAV is drawn to scale.

The analysis of the 6 traces during the test flights we observed a maximum off course mean of 15° with respect to the ideal trajectory and a mean deviation of 7.05° with a mean velocity of 0.617 m/s. For comparison we also plot a

trajectory of one run where the stabilization system is disabled. A comparison shows that our insect based neuronal stabilization system can reliably keep the UAV on course.

The vertical stabilization results shows that all the traces are constrained to a narrow margin of just 0.66 m within a trajectory of up to 8 seconds (fig. 7). The traces have an altitude mean of 1.676 m. and a standard deviation of 0.108 m., which has to be compared to the radius of the blimp of 0.3 m., i.e. the deviation is only about 18% of blimp height.

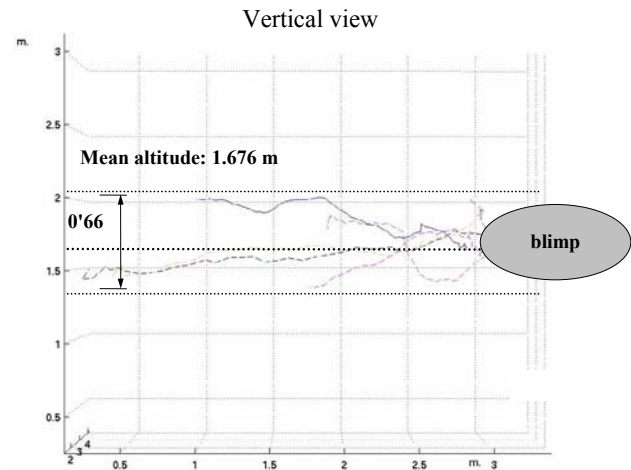


Figure 7: Lateral projection of the 6 test traces with balanced motor control onto the vertical plane. A mean altitude of 1.676 m. is maintained within a narrow interval of 0.66 m.

B. Collision detection and obstacle avoidance

The second visual pathway applied to the UAV is for collision avoidance: the Locust based LGMD model. As its biological equivalent this neuron starts to spike whenever it is stimulated by a looming stimulus, and it increases its activity as it gets closer to the object (fig. 8). The avoidance maneuver is triggered when the model response exceeds a fixed threshold. The responses of this model are very similar to the ones observed in its biological realization [3]

In a last experiment we evaluate how both visual system works in combination in a free-flight scenario (fig. 9). During this four minute flight, the robot controlled by the LGMD and the stabilization systems shows obstacle detection at a mean distance of 1.69 m. from the wall, i.e. within an interval of 1 m. and 2.7 m. with the longest distance in the test room being about 6.5 meters (fig. 9). The mean obstacle detection distance is calculated using the first spike of the LGMD model as the position at which the system detects the collision. However, this does not mean that an avoidance maneuver is triggered at that moment of the intrinsic structure of the neural model; a mean time of 3.9 seconds is required to perform the avoidance maneuver.

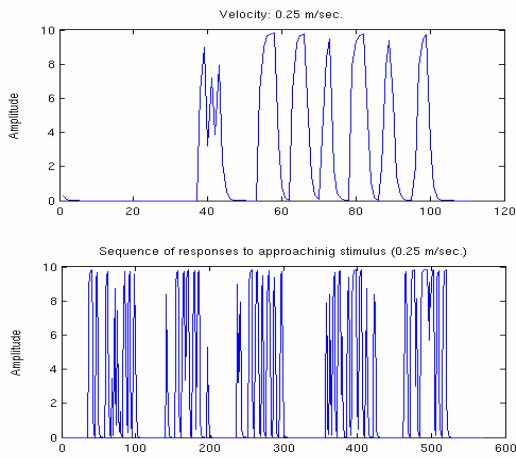


Figure 8: Responses of the LGMD model to approaching objects at 0.25 m/s. Single trace examples and a sequence of responses to the presentation of looming stimuli are plotted.

The response of the LGMD model is integrated over time in order to prevent the UAV from reacting to spurious activity and several spikes are required to activate an avoidance reaction. The duration of the avoidance maneuver is taken from the first event of spike of our neural model to the moment at which the system ceases to spike as a result of the loss of the looming stimulus. At this point, a trade-off between the speed of the UAV and the collision detection appears that is accurately reflected by the model: the higher the flight speed the faster the rate of looming of stimuli in front of the UAV and the less time is available to avoid it.

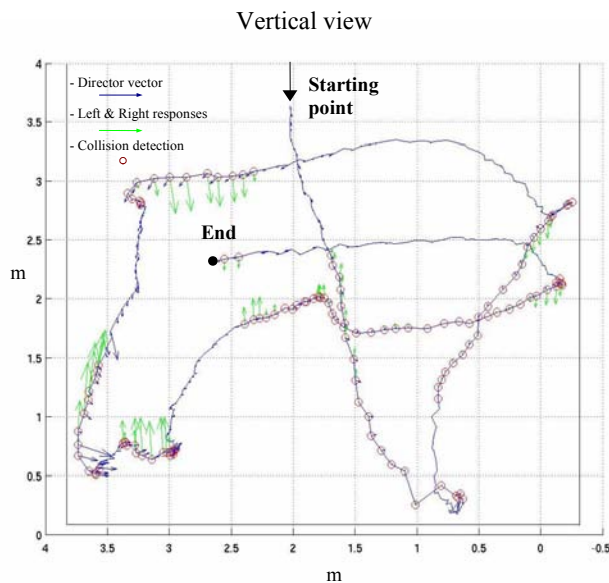


Figure 9: Trace of one minute flight of the UAV with both stabilization and collision avoidance systems enabled. Blue trace: the position of the UAV every 200 ms. Green arrows: the direction of the compensation responses to detected drift. Red dots: collision detection.

With these experiments, we have shown that reliable 3D flight control of a dirigible can be achieved using insect based reactive models. The behavior of the UAV is generated by an intrinsic hierarchical insect based neural model that goes from a simple photoreceptor to a wide-field visual neuron that is matched to a specific dynamic property of the world.

The simplicity of the model that only makes use of 2 reactive models to navigate (course stabilization, altitude compensation and collision avoidance) using visual flow is reflected in a lower computational cost, no use of additional memory or any training period. Although the model does not need to calculate physical distances to objects in the environment the environment, its responses are implicitly tuned to them because the responses of the motion sensitive cells depend on the ‘apparent’ motion and shape of the stimuli. Depending on the distance and size of the objects, similar movements are not seen the same way, i.e. for a constant object, if the motion is produced 1 meter or 10 meters away from the camera the perception of motion is not the same.

Using image correlations to detect the motion of the image makes this system quite robust in terms of the independency from the textures of the walls as long as any contrast is present in the image.

Other behaviorally similar models have been recently proposed in order to explain the behavior of the fruit fly *Drosophila Melanogaster* of the saccades triggered in order to avoid collisions [16]. A similar approach to our model has been applied recently to a terrestrial robot with good results [24]. Others have used a genetic algorithm to control a UAV where the fitness function looks for the maximization of forward motion [11]. As a result, they claim that the UAV is using collisions with the walls as a way to stabilize its trajectory and to maximize forward motion. Some good results can be obtained by using these techniques, but because of the high dependency on the training set, there is no control over the learned rules and the resulting behavior [6], the same system used for stabilization was also used for obstacle avoidance, looking at the asymmetries of the optical flow when an agent is getting close to a wall. In this case, a higher motion should be seen by a camera at the wall’s side than at the other side, using this factor as trigger of an avoidance reaction. This model, however, is not specifically designed to avoid collisions, and does not consider external factors such as the possibility of different textures on the walls, etc. This model essentially avoids collisions since it aims at maintaining the UAV flying at the same “apparent distance” from the reference walls. Nevertheless, in our approach we present two independent and task specific insect based models (fly and locust) that allow a blimp based UAV to successfully perform course stabilization, drift compensation and obstacle avoidance. As such this is one of the first demonstrations that such a biologically based neuronal model generalizes to control 3D flight in a real-world

environment.

In the future this system will be further enhanced with chemo-sensors to model the chemical search behavior of the moth. This model will be generalized to an outdoor system that will be used for chemical detection and environmental monitoring.

REFERENCES

- [1] Skafidas, A. Micro-controller Systems for a UAV, Auto Piloting and Camera Trigger System. ISSN 0280-316 X, 2002.
- [2] Autonomous Helicopter Project, <http://www-2.cs.cmu.edu/afs/cs/project/chopper/www/capability.html>.
- [3] Bermúdez i Badia, S. and Verschure, P.F.M.J. A Collision Avoidance Model Based on the Lobula Giant Movement Detector of the Locust. Proceedings of the International Joint Conference on Neural Networks 2004 (IJCNN04), p.1757, July 2004.
- [4] Egelhaaf, M.. On the neural basis of figure ground discrimination by relative motion in the visual system of the fly. I. Behavioral constraints imposed on the neuronal network and the role of optomotor system. Biol. Cybern. 52:123-140, 1985.
- [5] Egelhaaf, M. and Borst, Motion computation and visual orientation in flies. Comp. Biochem. Physiol. 104A:659-673, 1993.
- [6] Iida F. Goal-Directed Navigation of an Autonomous Flying Robot Using Biologically Inspired Cheap Vision. Proceedings of the 32nd ISR (International Symposium on Robotics), pp. 19-21, 2001.
- [7] Gabbiani, F., Krapp, H. G., Koch, C. & Laurent, G. Multiplicative computation in a visual neuron sensitive to looming. *Nature*, vol. 420, pp. 320-324, 2002.
- [8] Hatsopoulos, N., Gabbiani, F. & Laurent, G. Elementary computation of object approach by a wide-field visual neuron. *Science* 270, 1000-1003, 1995.
- [9] Hengstenberg, R.: Common visual response properties of giant vertical cells in the lobula plate of the blowfly *Calliphora*. *Journal of Comparative Physiology* 149, 179-193, 1982.
- [10] Linderman, J.P., Kern, R., Michaelis, C., Meyer, P., van Hateren J.H., Egelhaaf, M. FliMax, a novel stimulus device for panoramic and highspeed presentation of behaviourally generated optic flow. *Vision research* 43, pp. 779-791, 2003.
- [11] Zufferey, J., Floreano, D., van Leewen, M., and Merenda, T. Evolving Vision-Based Flying Robots. Proceedings of the 2nd International Workshop on Biologically Motivated Computer Vision, LNCS 2525, pp. 592-600, Berlin, Springer-Verlag. (BMCV'2002).
- [12] Borenstein, J. The HoverBot – An electrically Powered Flying Robot, Unpublished White Paper.
- [13] Douglas, J. K. and Strausfeld, N. J. Visual Motion-Detection Circuits in Flies: Parallel Direction- and Non-Direction-Sensitive Pathways between the Medulla and Lobula Plate. *The Journal of Neuroscience*, 16(15):4551-4562, 1996.
- [14] Kern, R., Lutterklas, M., Petercit, C., Lindemann, J.P., & Egelhaaf, M. Neural processing of behaviourally generated optic flow: Experiments and model simulations. *Network: Computations in Neural systems*, 2001.
- [15] Kern, R., Petercit, C., & Egelhaaf, M. Neural processing of naturalistic optic flow. *Journal of Neuroscience*, 21, 1-5, 2001.
- [16] Tammero, L. and Dickinson, M. H.. The influence of visual landscape on the flight behavior of fruit fly *Drosophila melanogaster*. *The Journal of Experimental Biology* 205, pp. 327-343, 2002.
- [17] Musial, M., Brandenburg, U.W., Hommel, G. Success of an Inexpensive System Design: The Flying Robot MARVIN. Technische Universität Berlin. <http://pdv.cs.tu-berlin.de/MARVIN/>.
- [18] Blanchard, M. and Verschure, P.F.M.J. Using a mobile robot to study locust collision avoidance responses. *International Journal of Neural Systems*, vol. 9, No. 5 405-410, 1999.
- [19] Blanchard, M, Rind, C. and Verschure, P.F.M.J. How accurate need sensory coding be for behaviour? Experiments using a mobile robot. *Neurocomputing* 38-40, pp. 1113-1119, 2001.
- [20] Ichikawa, M., Yamada, H. and Takeuchi, J. A flying robot controlled by a biologically inspired vision system. 8th International Conference on Neural Information Processing (ICONIP-2001), Shanghai, China, 2001.
- [21] Chan, P. and Wyeth, G. Self-Learning Visual Path Recognition. Proceedings of the Australian Conference on Robotics and Automation (ACRA'99). Brisbane, pp. 44-49, 1999.
- [22] Ready, D.F., Hanson, T.E., Benzer, S. Development of the *Drosophila* retina, a neurocrystalline lattice. *Dev Biol.* 1976 Oct 15;53(2):217-40, 1976.
- [23] Reichardt, Autocorrelation, a principle for the evaluation of sensory information by the central nervous system. In: *Sensory communication* (Rosenblith WA, ed) pp 303-317. New York: MIT Press-Wiley, 1961.
- [24] Harrison, R. A Low-Power Analog VLSI Visual Collision Detector. Proceedings of the Neural Information Processing Systems 2003, December 2003.
- [25] Rind, F.C. & Simmons, P.J. Orthopteran DMCD neuron: a reevaluation of responses to moving objects. I. Selective responses to approaching objects. *J. Neurophysiol.* 68, 1654-1666, 1992.
- [26] Schlotterer, G. R. Response of the locust descending movement detector neuron to rapidly approaching and withdrawing visual stimuli, *Can. J. Zool.* 55, 1372-1376, 1977.
- [27] Saripalli, S., Montgomery, J. F. and Sukhatme, G. S. Visually-guided landing of Unmanned Aerial Vehicle. <http://Citeseer.nj.nec.com/saripalli03visuallyguided.html>, 2003.
- [28] Netter, T., Franceschini, N. A Robotic Aircraft that follows Terrain using a Neuromorphic Eye. Proceedings of IEEE/RJS IROS2002, paper 593, 2002.
- [29] Bernardet, U., Blanchard, M. and Verschure, P.F.M.J. IQR: a distributed system for real-time real-world neuronal simulation. *Neurocomputing* 44-46: 1043-1048, 2002.
- [30] Braitenberg, V. Patterns of projections in the visual system of the fly. I. Retina-Lamina projections. *Experimental Brain Research*, vol. 3, pp. 227-298, 1967.
- [31] Hafner, V. V. and Salomon, R. Evolving Neural Controllers for Visual Navigation, Artificial Intelligence Laboratory, University of Zurich. Proceedings of the 2002 Congress on Evolutionary Computation, 2002.
- [32] Hafner, V. V., Kunz, H. and Pfeifer, R. An investigation into Obstacle Avoidance as an 'emergent' Behaviour from two Different Perspectives. Proceedings of the EPSRC/BBSRC International Workshop on Biologically-inspired Robotics. The legacy of W. Grey Walter, pp. 166-173. Bristol. 2002.